Analyst

Cite this: *Analyst*, 2011, **136**, 2726

www.rsc.org/analyst

PAPER

Probing chemical induced cellular stress by non-Faradaic electrochemical impedance spectroscopy using an *Escherichia coli* capacitive biochip†

Anjum Qureshi, Yasar Gurbuz and Javed H. Niazi*

Received 10th March 2011, Accepted 21st April 2011
DOI: 10.1039/c1an15202e

A new capacitive biochip was developed using carboxy-CNT activated gold interdigitated (GID) capacitors immobilized with *E. coli* cells for the detection of cellular stress caused by chemicals. Here, acetic acid, H_2O_2 and NaCl were employed as model chemicals to test the biochip and monitored the responses under AC electrical field by non-Faradaic electrochemical impedance spectroscopy (nFEIS). The electrical properties of *E. coli* cells under different stresses were studied based on the change in surface capacitance as a function of applied frequency (300–600 MHz) in a label-free and noninvasive manner. The capacitive response of the *E. coli* biochip under normal conditions exhibited characteristic dispersion peaks at 463 and 582 MHz frequencies. Deformation of these signature peaks determined the toxicity of chemicals to *E. coli* on the capacitive biochip. The *E. coli* cells were sensitive to, and severely affected by 166–498 mM (1–3%) acetic acid with declined capacitance responses. The *E. coli* biochip exposed to H_2O_2 exhibited adaptive responses at lower concentrations (<2%), while at a higher level (882 mM, 3%), the capacitance response declined due to oxidative toxicity in cells. However, *E. coli* cells were not severely affected by high NaCl levels (513–684 mM, 3–4%) as the cells tend to resist the salt stress. Our results demonstrated that the biochip response at a particular frequency enabled the determination of the severity of the stress imposed by chemicals and it can be potentially applied for monitoring unknown chemicals as an indicator of cytotoxicity.

1. Introduction

Microorganisms, such as bacteria can be used as biological sensing elements to determine the toxicity nature of a variety of chemicals.[1] Sensing the toxic nature of chemicals on bacterial cells enables the prediction of chemicals' potential to induce toxicity. A majority of chemicals are toxic in nature to living cells, these can be screened and predicted in mixtures.[2] Chemicals derived from pharmaceutical preparations, drugs, defense agents, contaminated environmental and food samples exhibit detrimental effects by causing cellular damage, such as oxidative, genotoxic, and metabolic stresses and thus are harmful to living organisms.[3–5] Living cells can be utilized to assess toxicological risk and to determine the toxic nature of chemicals. Bacterial cells can be an ideal choice as biological recognition elements because they respond to the external stress (stimuli), such as by toxic chemicals that lead to altered cellular dynamics, including metabolism, growth and cell surface charge distribution. Such responses can be utilized to predict the toxicity of chemicals.[6–10] The toxicity response of bacterial cells is often determined in terms of various stress responses. The stress responses in bacteria are classified into different types based on the nature of the chemical compound used to induce toxicity. For example, chemicals that induce various cellular toxicity responses through different modes such as by (i) metabolic/acid toxicity induced by chemicals such as, acetic acid, lactic acid, organic calcium salts, propionate, formate and drugs that influence intracellular accumulation of anions; (ii) oxidative toxicity induced by chemicals that produce reactive oxygen species (ROS) such as H_2O_2, hydroxyl radical (OH), superoxide anion (O_2^-), organic hydrogen peroxide (ROOH), peroxynitrite (OONO) and nitric oxide (NO); and (iii) osmotic stress induced by high concentrations of solutes including high levels of NaCl, osmolytes in the cytosol of cells subjected to osmotic stress, such as by carnitine, trehalose, glycerol, sucrose, proline, mannitol, and glycine-betaine[1,11,12] and others that induce genotoxic stress, and various cellular stress responses.[10,13]

Toxicity or the cell-killing property of a toxicant can be measured by following the cellular metabolic rate (*e.g.*, tetrazolium salt cleavage),[14] and the activity of a cytoplasmic enzyme (*e.g.*, lactate dehydrogenase).[15] The neutral red uptake assay (NR) and the total cellular protein assay are also the two principal methodologies for testing toxicity.[16] Other cytotoxicity methods involve the detection of pH changes in the neighborhood of cultured cells by a silicon microphysiometer[17] and the measurement of the barrier function of a cell layer (transcellular resistance) upon

Faculty of Engineering and Natural Sciences, Sabanci University, Orhanli, Tuzla, 34956, Istanbul, Turkey. E-mail: javed@sabanciuniv.edu; Fax: +90 216 483 9550; Tel: +90 216 483 9879

† Electronic supplementary information (ESI) available. See DOI: 10.1039/c1an15202e

exposure to test compounds.[18] The above methods are noninvasive that present quantitative measurements but require cell layers grown on membrane inserts. There have been several attempts on studying cytotoxicity by cellular and video imaging analysis and these require extensive data processing and only provide semi-quantitative results.[19,20] So far, the only successful commercially available microbial based toxicity screening method available under the name Microtox® is being used, which utilizes luminescent bacteria for measuring the effect of toxicants.[21] Such techniques may not be suitable for testing toxic gases (defense agents) and these are also required to depend on bacterial cells to express luminescent gene product and a luminometer.

Bacteria can respond to various cellular stresses under the AC electric field and the changes in electrical responses of bacteria to external stress can be captured or monitored by nFEIS. This can be accomplished by tethering live bacterial cells on GID electrodes as biological sensing surface (biochip). When toxic chemicals are exposed to these bacterial cells on a sensor surface, the cells respond to these chemicals that results in surface charge distribution, which can be measured by nFEIS against the AC electrical frequency sweep. As a result, the total charges present on the sensor surface polarize and relax depending on the specific frequency.[22] The change in response of bacterial cells on the sensor surface against the toxic/stress chemicals can be monitored. The sensitivity of the sensor surface can be enhanced by various surface chemistries, including modifying with highly reactive nanomaterials, such as carbon nanotubes (CNTs) as these possess unique structural, electronic and mechanical properties that make them a very attractive material for a wide range of applications in electrochemical sensing.[23,24] Recently, CNTs have been used as an electrode material for supercapacitors and also attracted much of attention because of their microscopic and macroscopic porous structures, electrochemical behavior, size and surface area that are important for the abundance of reaction sites, and provide a large-charge storage capacity and capacitance.[25–28] CNTs exhibit space charge polarization at the electrode–nanotube interface under the applied AC electrical frequency and possess superior power densities due to fast charge/discharge capabilities.[26,29]

Here, we demonstrated a new method to determine the toxicity of chemicals, that is a label-free and noninvasive approach that utilizes carboxy-CNT activated gold interdigitated capacitors immobilized with *E. coli* bacteria as biological sensing elements that do not require participation of any mediators by nFEIS. The sensitivity of the sensor surface was enhanced by covalent activation with carboxy-functionalized multiwalled CNTs that are less toxic than single walled CNTs. The proposed detection methodology is based on nFEIS, which can be used to screen various chemicals, toxic gases, pharmaceuticals, drugs, defense agents, environmental and food samples for the determination of chemicals' potential to cause cytotoxicity.

2. Experimental

Patterning GID array electrodes for fabrication of capacitor arrays

GID array electrodes were patterned on SiO_2 surfaces using the image reversal technique. In this process, the metal layers were patterned using the dual tone photoresist AZ5214E. A 2 μm thick AZ5214E photoresist was patterned with the help of a mask for a lift-off process in pure acetone as a solvent. Following this step, a very thin tungsten layer of 50–60 nm size was layered to improve the adhesion of gold on the SiO_2 film by DC sputter deposition and about 200–210 nm thick gold layer was deposited. The dimension of each electrode was 800 μm in length, 40 μm in width with a distance between two electrodes of 40 μm.[30] Each capacitor sensor contained 24-interdigitated gold electrodes within a total area of 3×3 mm^2. The surface characterization was performed using tapping mode Atomic Force Microscopy (AFM, Nanoscope) and by optical micrographs.

Immobilization of carboxy-CNTs on GID electrode capacitor arrays

The interdigitated gold electrode array capacitive chip was subjected to plasma cleaning and thoroughly washed with ethanol and dried under a stream of N_2 gas. A detailed procedure on covalent immobilization of carboxy-CNTs on capacitor chips is described and shown schematically in ESI, Fig. S1†.

Immobilization of *E. coli* cells on carboxy-CNTs activated GID capacitor arrays

The bacterial strain used in this study was *E. coli* DH5α. Actively growing *E. coli* cells were inoculated into fresh Luria Bertani (LB) medium and allowed to grow until the mid-logarithmic growth phase. The cells were then harvested by centrifugation at 1000*g* for 3 min and washed thrice with phosphate buffered saline (PBS) pH 7.2, and resuspended in the same buffer. The cell concentration was determined by colony counting after serial dilution followed by plating on LB-agar plates.

The carboxy-CNTs activated GID capacitor array chip was first rinsed with sterile distilled water and dried with pure nitrogen and incubated with a mixture of 100 mM of EDC and 50 mM NHS for 2 h. The chip was then removed, thoroughly washed with distilled water and incubated with 5 μL of bacterial suspension containing two different concentrations of 8.7×10^6 and 1.74×10^7 colony forming units (CFU) in PBS buffer, respectively for 2 h. A schematic diagram of bioconjugation of carboxy-CNTs activated GID capacitor chip is as shown in ESI, Fig. S2†. Optical micrographs were taken after immobilization of different concentrations of bacterial cells.

Exposure of stress chemicals on GID capacitor chips immobilized with *E. coli* (biochip)

The biochip was first washed with PBS buffer and preincubated at 37 °C for 1 h in a moist chamber. To a series of capacitor arrays of biochips, 5 μL of different concentrations of three stress chemicals, such as acetic acid (0–498 mM), hydrogen peroxide (0–882 mM) and sodium chloride (0–684 mM) as models were incubated on each capacitor for 1 h and 3 h, respectively at 37 °C in an array of capacitors previously activated with carboxy-CNTs and immobilized with *E. coli* cells. The response of cells was monitored under limited conditions in PBS buffer, pH 7.2.

Impedance/capacitance measurements

The impedance/capacitance responses were measured before and after the chemical treatment on the biochip surface by nFEIS. First, the capacitance/impedance was measured sequentially to ensure that chips remain active after every step that includes; (a) bare GID-capacitors, (b) after activation with carboxy-CNTs (c) after bioconjugation with *E. coli* cells, and finally (d) after exposure of biochip against different stress chemicals with different concentrations and times. For control, biochips were treated with only PBS buffer in place of stress chemicals (blank) and a negative control experiment was conducted using biochip containing heat-killed *E. coli* cells. For this, biochips containing immobilized *E. coli* cells (1.74×10^7) were subjected to heat treatment in an air-tight pre-heated humid chamber at 95 °C for 5 min followed by quickly freezing at −70 °C for 5 min, and thawing at 25 °C for 15 min. The above treatment process was repeated thrice and finally the biochip was dried under N_2 gas. The capacitance response in between the gold interdigitated electrodes was measured in the frequency range 50 MHz to 1 GHz using a Network Analyzer (Karl-Suss PM-5 RF Probe Station and Agilent-8720ES). The Network Analyzer was calibrated using SOLT (short-open-load-through) method. The impedance values were exported to MATLAB® software for the analysis. The absolute capacitance values of triplicate experiments were extracted at an effective frequency (*f*) range (300–600 MHz) and the standard deviations were shown as errors.

Results

The goal of this study was to develop a noninvasive, label-free capacitive biochip conjugated with viable *E. coli* cells (biochip) as biological recognition elements for determining the impact of chemicals to induce cellular stress by nFEIS. Model chemicals were used to test the response of the biochip such as, (a) acetic acid, which induces metabolic stress or acid shock,[31] (b) hydrogen peroxide, contributes to oxidative toxicity through ˙OH generation,[32] and (c) sodium chloride induces salt/osmotic stress.

Characterization of biochip sensor surface by AFM and optical micrographs

Surface topographical AFM images of a GID electrode capacitor before and after covalent attachment of carboxy-CNTs are shown in Fig. 1a–f. The bare GID electrode surface exhibited distribution of nanoparticles with varying diameters (~100 to 200 nm) and sizes (Fig. 1a and b). An AFM 3D height map image of the gold nanoparticles showed varying heights within scanned $4.2 \times 4.2\ \mu m^2$ GID electrode surface area (Fig. 1c). The activated bare GID electrode surface by covalent immobilization of carboxy-CNTs was confirmed by AFM images (Fig. 1d–f). After covalent immobilization of CNTs on the GID surface, the diameter of the carboxy-CNTs was determined to be in the range 50–70 nm (Fig. 1e). An AFM 3D height map image of carboxy-CNTs activated GID electrode surface showed the distribution and varying heights of immobilized carboxy-CNTs. The response of the bare GID capacitor surface was weakly charged and the activation of the sensor surface with carboxy-CNTs transformed it into a significantly enhanced charged surface (ESI, Fig. S3†). The activated sensor surface was then subjected to biofunctionalization for the development of biochip.

The GID capacitor surface activated with carboxy-CNTs was biofunctionalized by immobilizing with two different concentrations of *E. coli* DH5α cells (8.7×10^6 and 1.74×10^7 CFU) at which minimum non-specific adsorption occurred. Optical micrographs of carboxy-CNT activated electrode surface before and after immobilization of *E. coli* cells were examined (ESI, Fig. S4a–i†). The microscopic observation of chips showed densely and covalently immobilized *E. coli* cells on GID surface. The non-specific adsorption on the SiO_2 surface of the chips was also observed, which consistently persisted even after repeated washing of chips with PBS buffer. Higher cell concentration resulted in densely immobilized gold electrode surface that was clearly distinguishable from the lower cell density (ESI, Fig. S4d–i†). A 2D AFM image of a section of biochip showing immobilized *E. coli* cell is as shown in Fig.1g.

The capacitance responses of viable *E. coli* cells were measured as a function of scanned AC electrical frequency (50–600 MHz), and the cell density dependent increase in capacitance responses was observed (ESI, Fig. S5†). At low frequency (50–200 MHz), the capacitance response was less dependent on cell concentration while it becomes more dependent on the cell concentration beyond 200 MHz of applied frequency (ESI, Fig. S5†). Further higher cell-concentrations above 1.74×10^7 CFU showed more non-specific adsorption onto the SiO_2 surface. The cell concentration of 1.74×10^7 CFU yielded considerably enhanced responses with minimum non-specific adsorption on SiO_2 surface, and this concentration was chosen to study the cell responses to different chemical stresses under the AC electrical field. In previous studies, the effect of radiation at GHz frequencies on rat basophil leukemia cells was predominantly shown to be thermal in nature.[33] Therefore, considering this effect, in this study, the stress responses with the *E. coli* biochip sensor was monitored only with the applied AC electrical frequencies below 600 MHz ensuring that no thermal effect occurred during the capacitance measurements.

Electrical responses to chemical stresses by *E. coli* cells immobilized on biochip surface

The carboxy-CNT activated capacitor surfaces immobilized with *E. coli* cells (1.74×10^7 CFU) were treated with various concentrations of three model stress inducing chemicals, such as acetic acid (acid or metabolic stress), H_2O_2 (oxidative stress) and NaCl (salt stress) for 1 and 3 h as described in the Experimental section. The electrical responses of cells to different stresses were monitored using nFEIS after applying an AC electrical frequency sweep from 300 to 600 MHz. The concentration and time dependent responses of cells to different stresses were analyzed. In this study, the biochip responses were tested with concentrations of model chemicals above normal physiological levels that induce cellular stress responses. Fig. 2a and b show a schematic diagram of arrays of a capacitor biochip incubated with test chemicals and the response of *E. coli* cells with toxic chemicals.

The biochip was first tested by applying an AC electrical frequency sweep and extracted the data at an effective frequency (300–600 MHz). The capacitance response as a function of

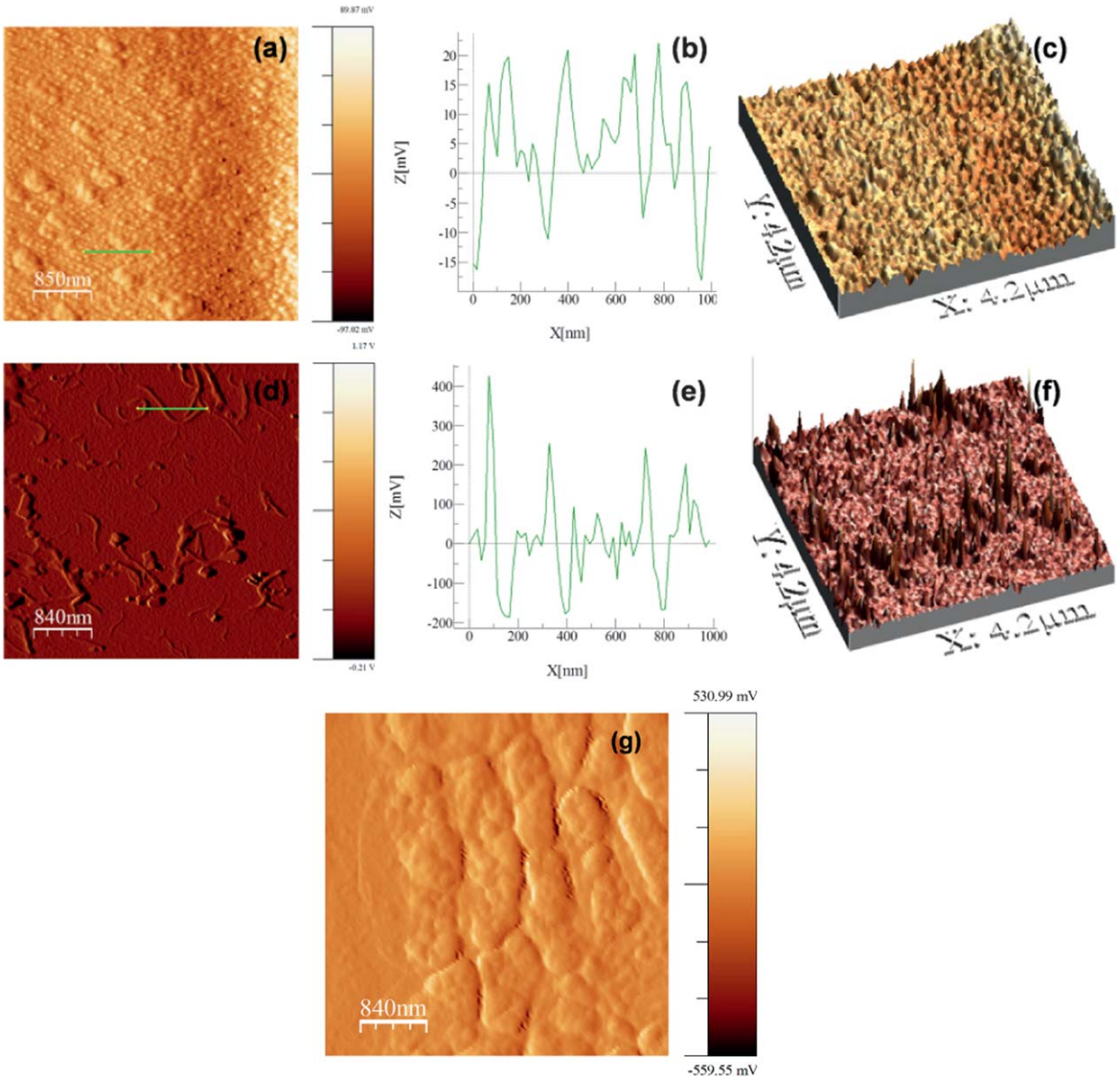

Fig. 1 Tapping-mode AFM images (within 4.2 × 4.2 μm^2 scan area) of (a) bare GID surface, (b) line plot surface profile of the selected green line region (1 μm length) in the tapping-mode AFM height image of bare GID surface, (c) 3D AFM topographical map of bare GID surface, (d) tapping-mode AFM height image of GID surface activated with carboxy-CNTs, (e) line plot surface profile of the selected green line region (1 μm length) in the tapping-mode AFM height image of GID electrode on capacitor surface activated with carboxy-CNTs, (f) 3D AFM topographical map of carboxy-CNT activated GID surface, and (g) a 2D tapping mode AFM image of a section (scan area 4.2 μm^2) of biochip showing immobilized *E. coli* cells.

applied frequency yielded two specific dispersion peaks at 463 and 582 MHz under normal conditions (untreated cells) (Fig. 3a). An independent control experiment was conducted using a biochip with heat-killed *E. coli* that did not show the characteristic dispersion peaks at 463 and 582 MHz, indicating that only viable cells exhibited the dispersion peaks (Fig. S5†). These two peaks represented a signature of cellular activity of immobilized *E. coli* under control/normal conditions. The *E. coli* biochip was treated with different concentrations of acetic acid to probe the sensor responses. The characteristic dispersion peaks were diminished due to the stress imposed by acetic acid at initial 1 h treatment. It was observed that the capacitive responses of the cells tend to decrease with increasing concentrations of acetic acid and its exposure time (1 h and 3 h) (Fig. 3a and b). This decrease in capacitance can be attributed to the transport activity of acetic acid across the cell membrane combined with the low pH of acetic acid that impaired the cell membrane function, which in turn may lower the cell's growth potential.[34] However, after 3 h of acetic acid stress, the cells exhibited a distinct response pattern in which the concentration above 166 mM (1%) of acetic acid showed persistent dispersion peak at 463 MHz but diminishing at 582 MHz. This result indicated that the cells undergo adaptation to the stress exerted by acetic acid over a period of time (here, at 3 h) as evidenced by the emergence or persistent dispersion peaks at 463 MHz and 582 MHz (Fig. 3b). After 3 h of acetic acid exposure, the cells were more sensitive to

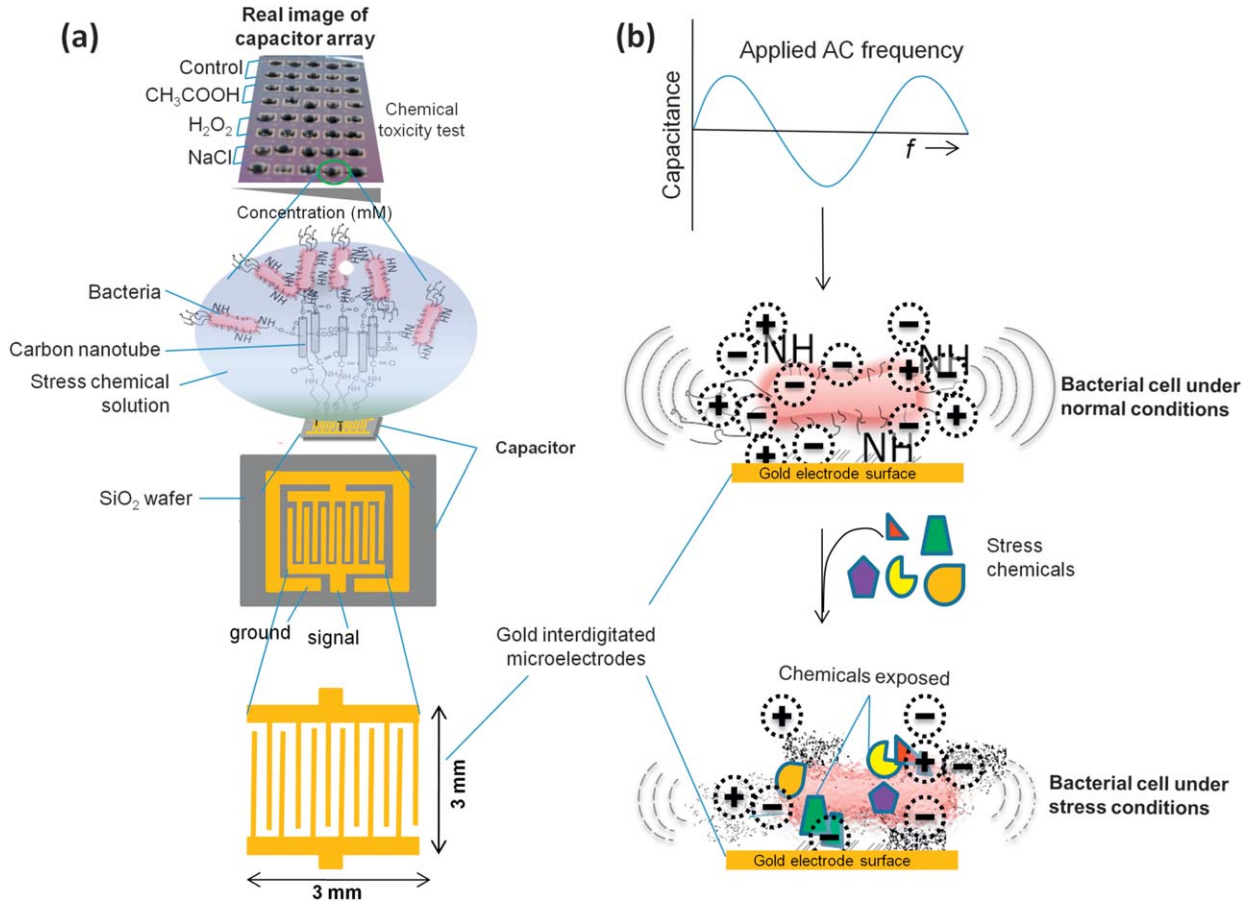

Fig. 2 Schematic representation of (a) capacitor array biochip immobilized with viable *E. coli* cells by tethering with carboxy-CNTs on gold interdigitated electrodes of each capacitor with a defined geometry and dimension; and (b) diagram showing the response of *E. coli* and surface charge distribution under the applied AC frequency in normal and chemical stress conditions.

acetic acid above 166 mM (1%) unlike at the initial 1 h exposure due to toxicity.

In order to study *E. coli* biochip responses to oxidative stress, the sensor surface was treated with different concentrations of H_2O_2 (0–882 mM, 0–3%) for 1 h and 3 h, respectively. *E. coli* cells treated with 294 mM (1%) of H_2O_2 resulted in a negligible change in capacitance response irrespective of exposure time but the disappearance of the characteristic dispersion peaks at 463 and 582 MHz was observed at 1 h, while they were persistent at 3 h, which is consistent with the fact that cells probably undergo

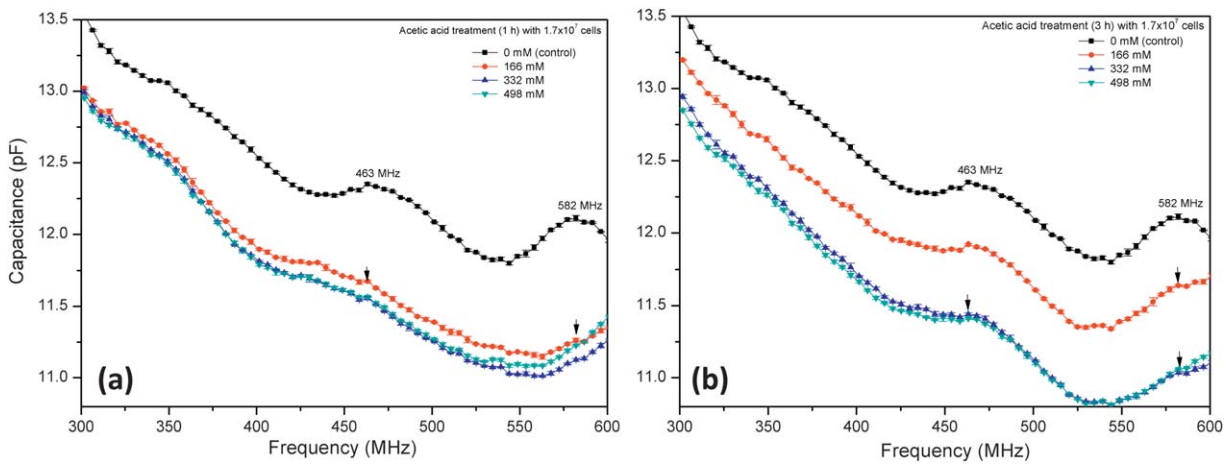

Fig. 3 Change in capacitance from *E. coli* capacitor biochip as a function of applied frequency (300–600 MHz) when exposed to different concentrations of acetic acid for (a) 1 h and (b) 3 h.

adaptation to stress over a 3 h time interval (Fig. 4a and b). It was observed from Fig. 4b that the cells showed higher capacitance responses with 588 mM (2%) of H_2O_2 and this response tends to decline noticeably with 882 mM (3%) at 3 h of exposure with disappearance of the characteristic dispersion peak at 582 MHz. This result indicated that the *E. coli* cells resisted low levels of oxidative toxicity that occurred by 294 mM (1%) H_2O_2. Whereas, at 588 mM (2%) H_2O_2 concentration, the cells displayed an adaptive response to the oxidizing agent, which indicates that the exposure to low levels of H_2O_2 allows bacterial cells to resist exposure to further toxic doses of H_2O_2 (Fig. 4b). However, at even higher levels (882 mM, 3% of H_2O_2), the sensor chip exhibited considerably reduced capacitance responses, suggesting that the cells failed to cope with the stress at the higher level of oxidative toxicity caused by 882 mM (3%) as opposed to 588 mM (2%) of H_2O_2 at 3 h of exposure.

The biochip was further tested by treating with yet another chemical, which is not toxic to cells, but at higher levels induces salt/osmotic stress. To test this, various concentrations of NaCl (0–684 mM, 0–4%) were incubated on the biochip to study the salt stress responses. It was observed that the cells experienced mild adaptive responses to 0–513 mM NaCl (0–3%) concentration at the initial 1 h of treatment and the cells tend to experience salt stress with 684 mM (4%) of NaCl concentration (Fig. 5a). In addition, at 1 h of salt exposure, the characteristic dispersion peaks were not prominent (Fig. 5a). At prolonged exposure of cells from 1 to 3 h, salt concentrations above 342 mM (2%) were found to induce salt stress while the cells were not affected by salt stress at lower concentrations (171–342 mM, 1–2%) (Fig. 5b).

Discussion

Living cells consist of a complex spatial arrangement of materials that have different electrical properties.[35] All bacteria have a cell membrane where oxidative phosphorylation occurs (in the absence of mitochondria). The cell membrane of bacteria is surrounded by a cell wall which is rigid and protects the cell from osmotic lysis or external environmental perturbations. In Gram negative bacteria, the outer membrane is made of lipopolysaccharides and proteins. The cell membrane consists of a lipid bilayer containing many proteins, where the lipid molecules are oriented with their polar groups facing outwards into the aqueous environment, and their hydrophobic hydrocarbon chains pointing inwards to form the membrane interior. The inside of a cell contains membrane covered particulates and many dissolved charged molecules. While the cell membrane is highly insulating, the interior of the cell is highly conductive. The observed dielectric properties of bacterial cells can be explained on the basis of a model consisting of a conducting cytoplasmic core, contained by a thin insulating membrane which in turn is surrounded by a porous conducting cell wall. At low frequencies, the capacitance response was less dependent on cell concentration/stress while it becomes more dependent above 300 MHz of applied frequency. It is well documented that cells exposed to an AC electrical frequency field result in the movement of layers of ions both inside and outside the surface of the cell wall effectively and becomes electrically polarized.[22] This polarization takes the form of electrical charges that are created on the external and interfacial surface (Fig. 2b), which influenced declining levels of capacitance beyond 300 MHz and thus relaxation behavior was observed (Fig. 3–5).

Characteristic dispersion peaks were observed from the untreated cells (control at 463 and 582 MHz frequencies) when exposed to an AC electrical field (300–600 MHz). Appearance of these characteristic dispersion peaks is a clear indication of the presence/attachment of viable *E. coli* under control conditions. When cells treated with different stresses with acetic acid, H_2O_2 and NaCl, the cells surface interacted with these stresses and showed the sensitivity toward adaptive/detrimental responses. The interaction of bacterial cells with stress probably yields a reduction of net surface charges and this resulted in the disappearance of the characteristic dispersion peaks. It is probably because of the loss of the cells' membrane function when exposed to stressed environment, and as a result, the membrane becomes more porous to ions,[22] and also causes extracytoplasmic protein misfolding.[36] It was possible to monitor the response of the biochip at a specific frequency as the response was dynamic to the frequency sweep from 300–600 MHz. Therefore, a frequency of 350 MHz was arbitrarily chosen and extracted the absolute capacitance values to elucidate the distinct responses of *E. coli*

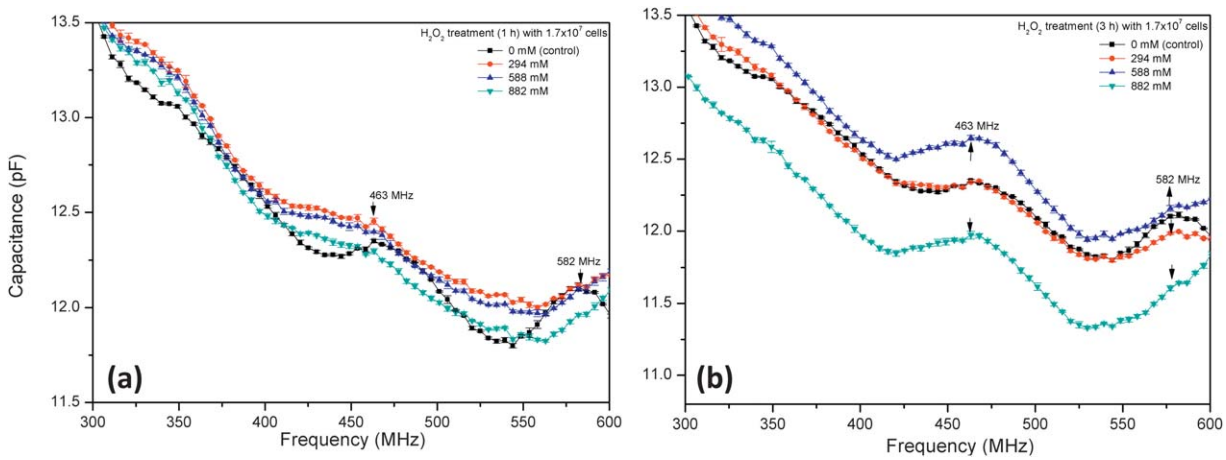

Fig. 4 Change in capacitance with *E. coli* capacitor biochip as a function of applied frequency (300–600 MHz) when exposed to different concentrations of H_2O_2 for (a) 1 h and (b) 3 h.

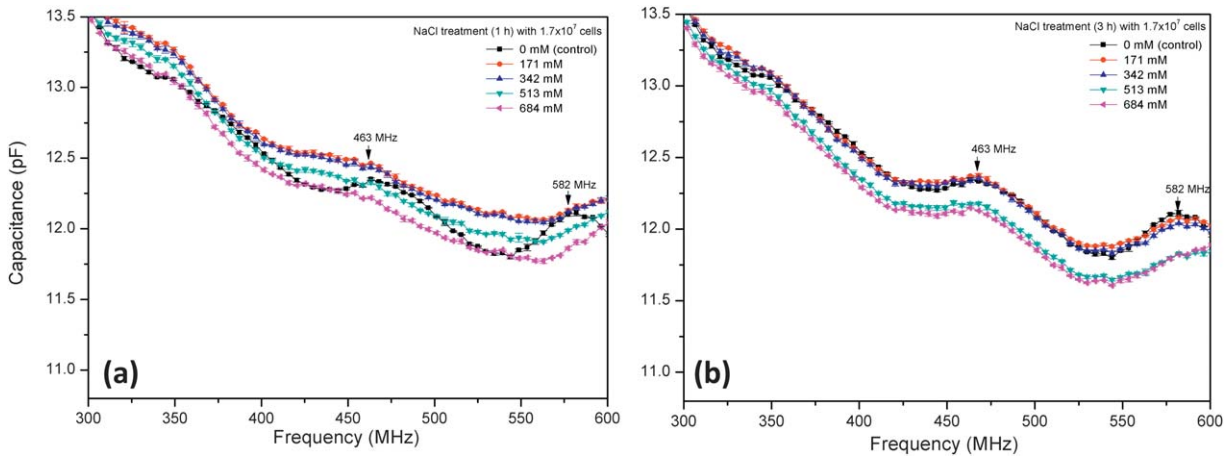

Fig. 5 Change in capacitance from *E. coli* capacitor biochip as a function of applied frequency (300–600 MHz) when exposed to different concentrations of NaCl for (a) 1 h and (b) 3 h.

cells against model stress chemicals with respect to their concentration and time. The severity of stress imposed by chemicals was color coded for visual inspection (Fig. 6a–c and insets).

The results showed that treatment with acetic acid resulted in declining capacitance responses, which is indicative of cells severely affected (shown red in the Fig. 6a) by acetic acid over time (1–3 h). In contrast, H_2O_2 at initial 1 h exposure exhibited adaptive responses (shown green in Fig. 6b) while at 3 h with 882 mM (3%), the cells were affected by oxidative stress imposed by high H_2O_2 (Fig. 6b), suggesting that 882 mM (3%) H_2O_2 is toxic to cells. A similar response was observed with the cells treated with various salt concentrations. It was found that at initial 1 h of NaCl exposure, cells tend to adapt by increasing the surface charge distribution and thus increase in capacitance. However, after 3 h of exposure, the capacitance tends to decrease with higher levels above 342 mM (2%) of NaCl because of the salt stress (Fig. 6c). It is clear from these results that cells are not severely affected by NaCl compared to that seen with acetic acid or H_2O_2 suggesting that cells can tolerate high salt levels but not high acetic acid or H_2O_2. This result is in agreement with previous studies where salt tolerance levels have been reported up to 1.1 M (~6.5%) NaCl for *E. coli*[37] and the cells could adapt to high salt concentrations for osmotolerance.[38,39]

E. coli are involved in the maintenance, adaptation and protection of the bacterial envelope in response to a variety of stressors.[40] It has been previously reported that the envelope stress response in *E. coli* is regulated by the two-component system comprised of membrane localized proteins such as BaeS and BaeR (BaeSR regulon) that govern the adaptive responses through efflux of toxic compounds and protects from other envelope perturbants, through unidentified mechanisms.[36,40] We here exploited this phenomenon to study the behavior of *E. coli* cells as biological recognition elements on biochips for monitoring the impact of stress inducing chemicals in a noninvasive method. Our results demonstrated the altered behavior of bacterial cells to stress chemicals under an AC electrical field in the bacterial biochip. The underlying hypothesis of the developed *E. coli* based capacitive biosensor is as follows: a complex bacterial cell surface consists of positive and negative charges

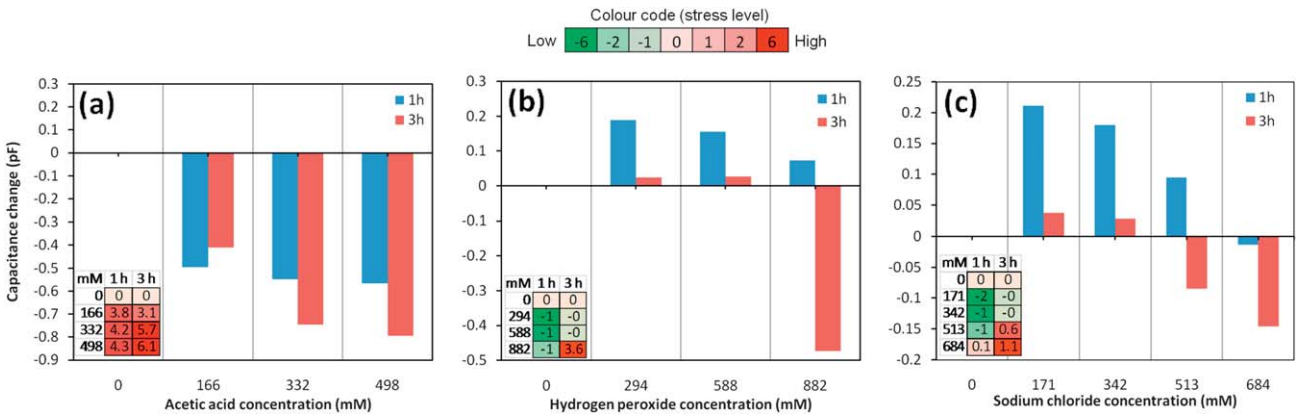

Fig. 6 Response of *E. coli* cells (immobilized on CNT activated sensor chip) as a function of different concentrations of (a) acetic acid (acid stress), (b) H_2O_2 (oxidative stress) and (c) NaCl (salt stress) at a constant AC electrical frequency (350 MHz) for 1 and 3 h treatment times. The inset tables show colour coded values determining the percent relative change in stress levels experienced by *E. coli* cells. The stress colour code scale indicates the severity of the stress levels in which green represents adaptation/resistance and red represents stress/toxicity.

that are constituted from the ionizable side chains of surface and pili-proteins in the outer membrane.[41,42] A typical bacterial cell, like a globular protein, exhibits surface charges that constitute an electric dipole.[43] The simplest molecular dipole of a bacterial cell (*E. coli*) consists of a pair of opposite electrical charges with magnitudes of $+q$ and $-q$ that are separated by a vector distance r. The molecular dipole moment m is given by the equation $m = qr$ (Fig. S6†). If a bacterial cell immobilized on a solid surface is exposed to any toxic chemical, the cells experience a stressful condition since the outer membrane becomes fragile or even disintegrated upon interaction with toxic chemicals and thus exhibit altered surface charge distribution.[44] In this study, we attempted to probe these changes when *E. coli* were exposed to model chemicals (acetic acid, H_2O_2 and NaCl) and successfully show the distinct responses to different chemicals in a concentration dependent manner and thus the results presented in this paper would provide knowledge on the toxicity of a given chemical.

Initially, the sensitivity of the capacitor sensor surface was tested using bare GID capacitor sensors. The sensitivity of these sensors was enhanced by activating the GID surface by carboxy-CNTs as described in the Experimental section. It was observed that the level of capacitance response was enhanced by several orders of magnitude (ESI, Fig. S3†). Therefore, all experiments were conducted using carboxy-CNTs activated sensor chips immobilized with *E. coli*. Here, immobilization of two *E. coli* concentrations (8.7×10^6 and 1.74×10^7 CFU) were chosen because at these concentrations there was minimum non-specific adsorption onto the SiO_2 surface. Further increase in cell concentration only yielded more non-specific adsorption on the sensor surface. For this, an additional step may be required during the chip fabrication process to prevent non-specific adsorption, for example, passivation of the SiO_2 surface by photoresist polymer such as SU-8, and leaving only the GID area open may enable efficient immobilization of bacterial cells and enhance the sensitivity. However, the method developed in this study can be extended to other cells (bacterial or mammalian) or tissues of specific function to probe the responses to external stimulus.

Conclusions

This paper demonstrates the development of a novel method for the detection of toxicity of chemicals on biological systems, using carboxy-CNT activated GID capacitor array chips immobilized with *E. coli*. The detection methodology is based on the nFEIS technique for monitoring the stress imposed by chemicals on bacterial cells. Using the biochip developed in this study is an effective means to understand and distinguish between toxic chemicals and non-toxic ones. The sensor platform developed can also be used to characterize the chemicals' nature including toxic gases to induce stress/toxic responses. An interesting feature of the developed *E. coli* biochip is the use of the dispersion peaks at 463 and 582 MHz as signatures of activity of *E. coli* and the change in capacitance levels at these frequencies would determine the toxic nature of stress chemical.

Until recently, the only successful commercially available microbial based toxicity screening method available (Microtox®), which utilizes luminescent bacteria for measuring the effect of toxicants has been adapted by US environmental protection agency (EPA) as a standard assay. However, this technique may seem incompatible for toxic gases (usually defense agents), or for changes in external physical factors such as, pH and temperature. One of the main advantages of using the developed biochip is that the non-specific signal can be avoided immediately after the treatment by simply washing away the biochip surface with appropriate buffer and measuring the capacitance under dry conditions. The detection methodology and biochip developed, therefore, finds advantages in testing different physical forms of stress agents (including gaseous, solid or liquid phase) and that it can be extended to determining potential toxicity and screening for monitoring environmental contaminants and food samples. However, there are a few challenges that need to be addressed in order to improve sensitivity through (a) better design of gold interdigitated electrodes, (b) geometry, (c) an additional step of passivation layer formation on the SiO_2 surface is required during chip fabrication to prevent non-specific adsorption of cells on the SiO_2 surface, (d) surface chemistry, (e) signal-to-noise ratio, and (f) bio-chemical assay conditions.

Acknowledgements

We thank Ozge Malay and Taner Aytun of Material Science and Engineering, Sabanci University for helping in obtaining AFM images. We also thank Bulent Koroglu and Saravan Kallempudi for their valuable contributions to the processing of devices and chip fabrication. The author A.Q. is thankful to TUBITAK Research Fellowship for Foreign Citizens (B.02.1.TBT.0.06.01-216.01-220/175).

References

1 J. H. Niazi, B. C. Kim, J. M. Ahn and M. B. Gu, *Biosens. Bioelectron.*, 2008, **24**, 670–675.
2 R. Altenburger, T. Backhaus, W. Boedeker, M. Faust, M. Scholze and L. Grimme, *Environ. Toxicol. Chem.*, 2000, **19**, 2341–2347.
3 H. Rosenkranz and A. Cunningham, *Regul. Toxicol. Pharmacol.*, 2001, **33**, 313–318.
4 O. Bechor, D. Smulski, T. Van Dyk, R. LaRossa and S. Belkin, *J. Biotechnol.*, 2002, **94**, 125–132.
5 E. Dybing, J. Doe, J. Groten, J. Kleiner, J. O'Brien, A. Renwick, J. Schlatter, P. Steinberg, A. Tritscher and R. Walker, *Food Chem. Toxicol.*, 2002, **40**, 237–282.
6 J. L. Ramos, T. Krell, C. Daniels, A. Segura and E. Duque, *Curr. Opin. Microbiol.*, 2009, **12**, 215–220.
7 S. Belkin, D. R. Smulski, S. Dadon, A. C. Vollmer, T. K. Van Dyk and R. A. Larossa, *Water Res.*, 1997, **31**, 3009–3016.
8 S. Isken and J. A. M. de Bont, *Extremophiles*, 1998, **2**, 229–238.
9 M. B. Gu and S. H. Choi, *Water Sci. Technol.*, 2001, **43**, 147–154.
10 J. H. Lee, C. H. Youn, B. C. Kim and M. B. Gu, *Biosens. Bioelectron.*, 2007, **22**, 2223–2229.
11 V. Capozzi, D. Fiocco, M. L. Amodio, A. Gallone and G. Spano, *Int. J. Mol. Sci.*, 2009, **10**, 3076–3105.
12 L. Vorob'eva, *Appl. Biochem. Microbiol.*, 2004, **40**, 217–224.
13 J. M. Ahn, E. T. Hwang, C. H. Youn, D. L. Banu, B. C. Kim, J. H. Niazi and M. B. Gu, *Biosens. Bioelectron.*, 2009, **25**, 767–772.
14 M. Berridge, A. Tan, K. McCOY and R. Wang, *Biochemica*, 1996, **4**, 14–19.
15 A. de Luca, M. Weller and A. Fontana, *J. Neurosci.*, 1996, **16**, 4174–4185.
16 C. Xiao, B. Lachance, G. Sunahara and J. Luong, *Anal. Chem.*, 2002, **74**, 5748–5753.
17 J. Parce, J. Owicki, K. Kercso, G. Sigal, H. Wada, V. Muir, L. Bousse, K. Ross, B. Sikic and H. McConnell, *Science*, 1989, **246**, 243–247.

18 A. Pasternak and W. Miller, *Biotechnol. Bioeng.*, 1996, **50**, 568–579.
19 D. Weiss, *Mol. Toxicol.*, 1987, **1**, 465–488.
20 W. Maile, T. Lindl and D. Weiss, *Mol. Toxicol.*, 1987, **1**, 427.
21 J. Chang, P. Taylor and F. Leach, *Bull. Environ. Contam. Toxicol.*, 1981, **26**, 150–156.
22 C. E. Hodgson and R. Pethig, *Clin. Chem.*, 1998, **44**, 2049–2051.
23 M. Zhang, A. Smith and W. Gorski, *Anal. Chem.*, 2004, **76**, 5045–5050.
24 G. Rivas, M. Rubianes, M. Rodriguez, N. Ferreyra, G. Luque, M. Pedano, S. Miscoria and C. Parrado, *Talanta*, 2007, **74**, 291–307.
25 J. N. Barisci, G. G. Wallace and R. H. Baughman, *J. Electrochem. Soc.*, 2000, **147**, 4580–4583.
26 K. H. An, W. S. Kim, Y. S. Park, Y. C. Choi, S. M. Lee, D. C. Chung, D. J. Bae, S. C. Lim and Y. H. Lee, *Adv. Mater.*, 2001, **13**, 497–500.
27 S. Kang, M. Herzberg, D. F. Rodrigues and M. Elimelech, *Langmuir*, 2008, **24**, 6409–6413.
28 B. J. Yoon, S. H. Jeong, K. H. Lee, H. S. Kim, C. G. Park and J. H. Han, *Chem. Phys. Lett.*, 2004, **388**, 170–174.
29 R. Basu and G. S. Iannacchione, *J. Appl. Phys.*, 2008, **104**, 114107.
30 A. Qureshi, Y. Gurbuz, S. Kallempudi and J. H. Niazi, *Phys. Chem. Chem. Phys.*, 2010, **12**, 9176–9182.
31 C. Kirkpatrick, L. Maurer, N. Oyelakin, Y. Yoncheva, R. Maurer and J. Slonczewski, *J. Bacteriol.*, 2001, **183**, 6466–6477.
32 J. Greenberg and B. Demple, *J. Bacteriol.*, 1989, **171**, 3933–3939.
33 M. Olapinski, S. Manus, N. Fertig and F. Simmel, *Biosens. Bioelectron.*, 2008, **23**, 872–878.
34 T. Warnecke and R. Gill, *Microb. Cell Fact.*, 2005, **4**, 25.
35 L. Yang and R. Bashir, *Biotechnol. Adv.*, 2008, **26**, 135–150.
36 R. G. Raffa and T. L. Raivio, *Mol. Microbiol.*, 2002, **45**, 1599–1611.
37 K. Glass, J. Loeffelholz, J. Ford and M. Doyle, *Appl. Environ. Microbiol.*, 1992, **58**, 2513–2516.
38 B. Landfald and A. Strom, *J. Bacteriol.*, 1986, **165**, 849.
39 U. Dinnbier, E. Limpinsel, R. Schmid and E. Bakker, *Arch. Microbiol.*, 1988, **150**, 348–357.
40 T. L. Raivio, *Mol. Microbiol.*, 2005, **56**, 1119–1128.
41 J. S. Dickson and M. Koohmaraie, *Appl. Environ. Microbiol.*, 1989, **55**, 832–836.
42 K. E. Magnusson, J. Davies, T. Grundstrom, E. Kihlstrom and S. Normark, *Scand. J. Infect. Dis., Suppl.*, 1980, **24**, 135–140.
43 A. Qureshi, J. Niazi, S. Kallempudi and Y. Gurbuz, *Biosens. Bioelectron.*, 2010, **25**, 2318–2323.
44 N. Narayanan and C. P. Chou, *Biotechnol. Prog.*, 2008, **24**, 293–301.